Short-Fiber-Reinforced Styrene–Butadiene Rubber Composites

V. M. MURTY and S. K. DE, *Rubber Technology Centre, Indian Institute of Technology, Kharagpur-721302, India*

Synopsis

Processing characteristics, anisotropic swelling, and mechanical properties of short-jute-fiber- and short-glass-fiber-reinforced styrene–butadiene rubber (SBR) composites have been studied both in the presence and absence of carbon black. Tensile and tear fracture surfaces of the composites have been studied using scanning electron microscopy (SEM) in order to assess the failure criteria. The effects of bonding agent, carbon black, jute fiber, and glass fiber on the fracture mode of the composites have also been studied. It has been found that jute fiber offers good reinforcement to SBR as compared to glass fibers. The poor performance of glass fibers as reinforcing agent is found to be mainly due to fiber breakage and poor bonding between fiber and rubber. Tensile strength of the fiber–SBR composites increases with the increase in fiber loading in the absence of carbon black. However, in the presence of carbon black a minimum was observed in the variation of strength against fiber loading. SEM studies indicate that fracture mode depends not on the nature of the fiber but on the adhesion between the fiber and the matrix.

INTRODUCTION

Although the use of short fibers in rubber compounding has started long ago when solkafloc was used to assist processing and for economic considerations,[1] it is only recently that short fibers have attracted the attention of several researchers because of their advantages in mechanical properties, good dispersion, and good adhesion to rubber matrix.[2-5] Compounding of rubbers with short fibers of synthetic type has been studied by O'Connor.[6] De and co-workers have reported their results on the studies of jute fiber reinforced natural rubber (NR) and carboxylated nitrile rubber (XNBR).[7-9] Setua and De have studied short-silk-fiber-reinforced NR composites[10] and Murty has studied short-glass-fiber-reinforced NR composites.[11] Murty, Bhowmick, and De have studied the failure of short-glass-fiber-reinforced NR by scanning electron microscopy.[12]

In the present paper we report the results of our investigations on processing and mechanical properties of SBR reinforced by short jute fiber and short glass fiber. The effects of bonding agent and reinforcing carbon black have been studied. Failure surfaces have been examined by scanning electron microscopy (SEM).

EXPERIMENTAL

Jute fiber (Grade TD1) as supplied by Indian Jute Industries Research Association, Calcutta, chopped to 6 mm length and treated chopped glass fiber of length 9 mm (rubber compatible fiber strands) as supplied by Fiberglass Pilk-

Journal of Applied Polymer Science, Vol. 29, 1355–1368 (1984)
 CCC 0021-8995/84/041355-14$04.00

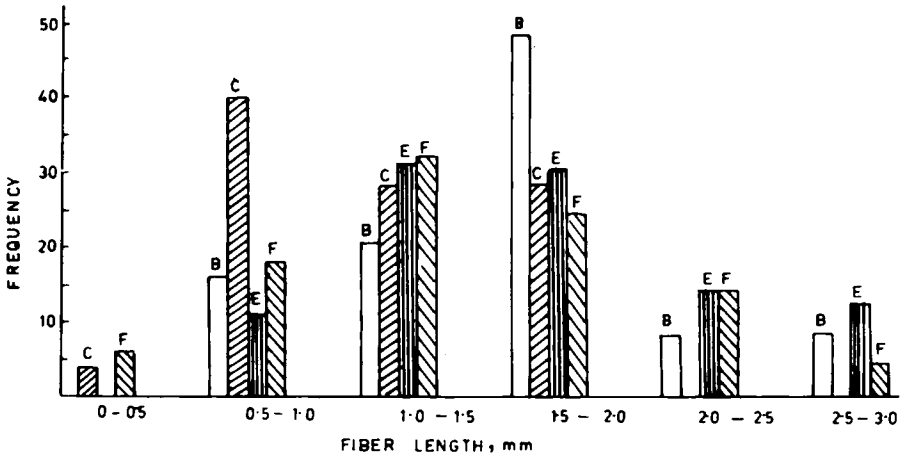

Fig. 1. Histogram showing the distribution of fiber length of jute fiber after mixing:

Mix no.	Avg L (mm)	Avg diam (mm)
B	1.59	0.04
C	1.06	0.03
E	1.60	0.04
F	1.45	0.04

ington Ltd., Bombay, were used in the present study. Mixing was done on an open mixing mill (15 cm × 33 cm). Nip gap, mill roll speed ratio, and the number of passes were kept the same for all mixes. In the case of jute fiber the fiber was mixed first with SBR, and the remaining ingredients were added later to ensure better dispersion of the fiber. The dispersion of glass fiber is good, and it is added to the compound after the addition of resorcinol and stearic acid. Resorcinol and stearic acid were mixed in their molten state. Finely ground hexamethylene tetraamine (hexa) was used.

In order to study fiber breakage, the fibers were extracted from the compound by dissolving the compound in benzene, and their length and diameter were measured using an optical microscope. Green strength was determined using the method developed by Foldi.[13] The compound was pressed at 120°C for 2 min, and the strength at yield point was taken as the green strength. The mill shrinkage was determined according to ASTM D 1917-62T.

Rectangular specimens with length along the direction of fiber length were cut from the sheets and swollen in benzene at room temperature for 3 days to determine anisotropic swelling of the composites. Percent increments in length and width were determined.

Mixes were vulcanized at 150°C to their respective optimum cure times as obtained from Monsanto Rheometer R-100. The method of preparation of vulcanizates was the same as reported earlier.[14] All the tests were carried out according to ASTM standards as given earlier.[7] Excepting hardness, resilience, and abrasion resistance, the tests were carried out both along and across the grain

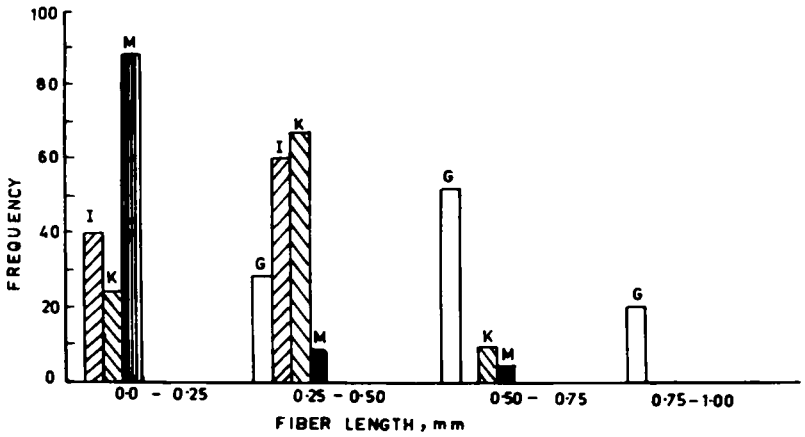

Fig. 2. Histogram showing the distribution of fiber length of glass fiber after mixing:

Mix no.	Avg L (mm)	Avg diam (mm)
G	0.58	0.08
I	0.30	0.01
K	0.34	0.01
M	0.19	0.01
Original fiber	9.04	0.33

direction. The fiber orientation was maximum along the grain direction. In the case of hardness and resilience, the direction of fiber alignment is normal to the direction of application of the load and the orientation of fiber is considered to be random in abrasion testing.

The samples were aged for 48 h at 100°C in an aging oven (Blue M, FC 712), to determine the aging resistance of the composites.

The fracture surfaces were sputter-coated with gold, and the SEM studies were done using a Philips 500 Model SEM.

RESULTS AND DISCUSSION

Processing Characteristics. Both types of fiber were found to undergo breakage during mixing, and the breakage pattern is reported in Figures 1 and 2. The aspect ratio of jute fiber decreased from 150 to 40 (at 10 phr loading) and to 28 (at 40 phr loading). Addition of 20 phr carbon black does not affect the fiber breakage any more. However, the diameter of jute fiber remained the same during mixing.

In the case of glass fiber the breakage is very severe and is dependent both on the loading of fiber and also on the presence of carbon black. Maximum decrease in fiber length is about 50 times and is observed for the mix containing 40 phr carbon black and 75 phr short glass fiber. The original diameter in the case of glass fiber has also decreased during mixing with the extent depending on the loading of fiber and the presence of carbon black. Similar observations for glass fiber were reported earlier.[6,11,15] Scanning electron microscopic observation

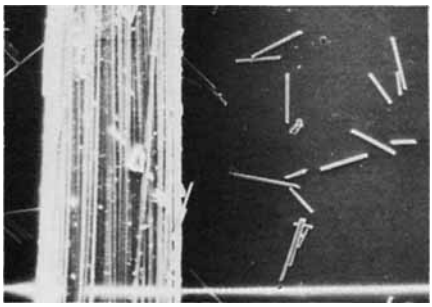

Fig. 3(a). Photomicrograph showing the length of original and broken glass fiber (12×).

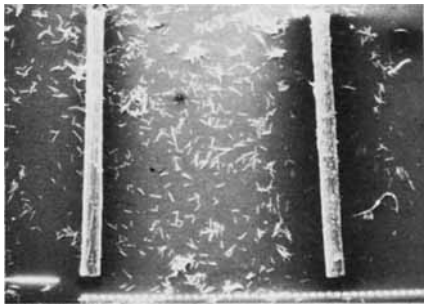

Fig. 3(b). Photomicrograph showing the diameter of original and broken glass fiber (100×).

of the original and broken glass fibers [photomicrographs, Figs. 3(a) and 3(b)] reveal that many individual filaments are put together in the raw state and coated with a bonding agent based on resorcinol–formaldehyde–latex system. These strands, because of poor adhering property of sizing and the shear force during mixing, might have separated leaving broken individual filaments to disperse in the rubber matrix. This may be the reason for the poor bonding between glass fiber and rubber matrix.

Addition of short fibers reduces the elasticity of rubber, and, therefore, when the compounded sheet is cut on the open roll, the elastic recovery or the shrinkage of the uncured sheet is restricted by the presence of fibers. This is clearly seen

TABLE I
Processing Characteristics[a]

Jute fiber (phr)	0	10	30	—	—	—	0	10	30	0	—	—
Glass fiber (phr)	—	—	—	10	25	75	—	—	—	0	10	25
Carbon black (N 330) (phr)	0	0	0	0	0	0	20	20	20	40	40	40
Mill shrinkage (%)	51	24	2	30	25	20	47	22	4	40	29	21
Green strength (MPa)	—	0.33	1.03	0.30	—	0.84	0.24	—	1.81	0.38	0.48	0.71

[a] The base recipe is the same as that given in Table III.

TABLE II
Anisotropic Swelling[a]

Jute fiber (phr)	Glass fiber (phr)	Carbon black (N 330) (phr)	Percent swell in length	Percent swell in width
0	0	0	75	68
10	—	0	38	66
30	—	0	4	44
0	0	20	63	56
10	—	20	33	37
30	—	20	2	37
—	10	0	65	62
—	25	0	39	54
—	75	0	13	53
—	0	40	46	50
—	10	40	42	43
—	25	40	8	60
—	75	40	23	21

[a] The base recipe is the same as that given in Table III.

from the values of mill shrinkage reported in Table I. It is also true that the extent of restriction depends on the fiber characteristics. That is why the mill shrinkage values are higher for glass fiber–SBR compounds in which case the breakage of fiber is high. Carbon black does not contribute much to the mill shrinkage.

Green strength is improved by the addition of short fibers and the presence of carbon black enhances the property. Similar observations have been made earlier by Foldi[13] and De and co-workers.[8,10] In general jute fiber offers better green strength compared to glass fiber.

Anisotropic Swelling. The swelling characteristics of short-fiber-reinforced rubber vulcanizates have been used to correlate mechanical properties with fiber orientation.[16,17] Swelling is considered to be a uniform restrictive force induced on the sample. Because of the anisotropic nature of the fiber–rubber composites, the swelling is restricted in the direction of fiber alignment and consequently the swelling becomes anisotropic. From the results in Table II it can be seen that both jute and glass fiber–SBR composites display anisotropic nature of swelling. Jute fibers exhibit higher anisotropy, particularly at higher loadings both in the presence and absence of carbon black. But at lower loadings the anisotropy is not considerable especially in the case of jute fiber–carbon black system, possibly due to competitive isotropic swelling restriction by carbon black. The lesser anisotropy in the case of glass fiber may be attributed to poor bonding between glass fiber and the rubber matrix. The anisotropy in swelling is absent for the mix M (containing 40 phr carbon black, 75 phr glass fiber). As the fiber length becomes very small, carbon black may have a more prominent effect on swelling than the fiber.

Mechanical Properties. Mechanical properties of jute and glass fiber-SBR composites are given in Tables III and IV, respectively. It is generally known[18] that the tensile strength of short-fiber-reinforced composites exhibit a minimum with the variation of fiber loading. Both jute-fiber- and glass-fiber-reinforced natural rubber composites have shown such minima.[7,8,11] But SBR composites do not show any minimum, and the tensile strength continuously increases with

TABLE III
Physical Properties of Vulcanizates[a,b]

Jute fiber (phr)	—	0	10	30	0	10	30
Carbon black (N 330) (phr)	—	0	0	0	20	20	20
Tensile strength (MPa)	L	3.74	3.88	6.16	12.39	5.85	7.19
	T	3.85	4.07	3.22	11.82	5.25	5.73
Modulus at 100%	L	0.08	2.66	—	1.33	2.96	—
elongation (MPa)	T	0.09	2.67	3.08	1.55	1.92	4.19
Elongation at break (%)	L	550	460	40	560	270	b
	T	550	455	410	560	470	450
Tear strength (kN/m)	L	16.6	26.6	32.7	38.7	48.3	60.0
	T	12.6	29.8	36.3	32.6	55.3	60.4
Hardness (Shore A)	—	40	65	80	55	80	90
Resilience (%)	—	46	51	47	46	46	44
Heat buildup, ΔT (°C)	L	15	—	44	14	45	47
	T	15	35	46	—	41	51
Compression set (%)	L	49	41	53	51	36	34
	T	50	44	47	53	39	36
Flex cracking resistance	L	16.6	1.7	1.7	40	3.4	0.6
to failure (kcycles)	T	18.0	1.7	1.7	40	4.4	0.9
Abrasion loss	—	2.12	2.18	2.65	0.94	1.40	1.47
V_r[c] (cc/500 rev)		0.155	0.169	0.208	0.165	0.206	0.207
Percentage retention of properties after aging at 100°C for 48 h							
Tensile strength	L	41	83	100	67	128	161
Tear strength	L	91	58	97	86	67	65
Elongation at break	L	46	22	133	45	20	40

[a] Base recipe: SBR 100, ZnO 5, stearic acid 2, resorcinol 5, silica 5, CBS 1, sulfur 2, hexa, 3.2.

[b] The sample has yielded at 20% elongation, with elongation at break 500% and strength at break 7.0 MPa.

[c] The samples were swollen in benzene for 48 h at 35 ± 2°C.

TABLE IV
Physical Properties of Vulcanizates[a]

		G	H	I	J	K	L	M
Glass fiber (phr)	—	10	25	75	0	10	25	75
Carbon black (N 330) (phr)	—	0	0	0	40	40	40	40
Tensile strength (MPa)	L	3.76	3.64	5.09	14.85	13.10	11.75	10.26
	T	3.80	4.44	4.33	14.55	12.84	10.55	7.87
Modulus at 100%	L	1.77	3.00	—	2.22	4.20	6.81	7.65
elongation (MPa)	T	1.65	2.55	3.10	2.20	3.34	3.49	3.54
Elongation at break (%)	L	490	440	70	430	370	260	320
	T	500	500	400	420	400	380	325
Tear strength (kN/m)	L	21.8	26.6	31.3	44.3	56.0	66.7	52.3
	T	23.6	31.3	36.6	40.4	57.4	56.4	43.0
Hardness (Shore A)	—	55	65	80	65	75	82	90
Resilience (%)	—	56	56	50	37	47	54	65
Heat buildup, ΔT (°C)	L	35	44	48	20	51	54	65
	T	33	36	48	21	58	54	59
Compression set (%)	L	28	23	36	46	45	43	37
	T	29	30	36	42	43	39	48
Flex cracking resistance to failure (kcycles)	L	4.3	2.5	0.5	30.0	7.0	3.9	0.3
	T	6.5	5.0	1.0	22.5	7.0	5.7	0.7
Abrasion loss	—	1.67	1.93	2.23	0.70	0.61	0.87	1.22
V_r[b] (cc/500 rev)	—	0.184	0.199	0.208	0.173	0.191	0.225	0.221
Percentage retention of properties after aging at 100°C for 48 h								
Tensile strength	L	91	103	127	78	74	109	162
Tear strength	L	79	146	78	99	50	54	73
Elongation at break	L	41	14	71	10	27	27	9

[a] Base recipe: SBR 100, ZnO 5, stearic acid 2, resorcinol 5, silica 5, hexa 3.2, CBS 1, sulfur 2.
[b] The samples were swollen in benzene for 48 h at 35 ± 2°C.

TABLE V
Formulation of the Mixes Used for SEM Studies

	S	T	U	V	W	X	Y	Z
SBR 1502	100	100	100	100	100	100	100	100
ZnO	5	5	5	5	5	5	5	5
Stearic acid	2	2	2	2	2	2	2	2
Resorcinol	0	0	5	5	5	5	5	5
Silica	5	5	5	5	5	5	5	5
Jute fiber	0	0	0	0	30	0	0	30
Glass fiber	0	0	0	25	0	50	25	0
Carbon black (N 330)	0	20	0	0	0	0	40	20
Oil	0	2	0	0	0	0	4	2
Hexa	0	0	3.2	3.2	3.2	3.2	3.2	3.2
CBS	1	1	1	1	1	1	1	1
Sulfur	2	2	2	2	2	2	2	2
Tensile strength (MPa)	2.24	14.32	3.74	3.00	6.16	4.70	11.75	7.19
Tear strength (kN/m)	11.9	34.01	16.6	26.6	32.7	—	66.7	70.0

fiber concentration. The concept of critical volume of fiber loading at which fiber–rubber composites exhibit minimum tensile arises from the net result of two factors[19]: (a) the weakening of the rubber matrix strength (for example, NR due to its crystallinity) by the presence insufficient quantity of fibers; (b) the contribution of the fibers towards the increase in composite strength (where the load transfer area between the fibers and rubber becomes important, which is mainly determined by the aspect ratio and adhesion). In the case of SBR,

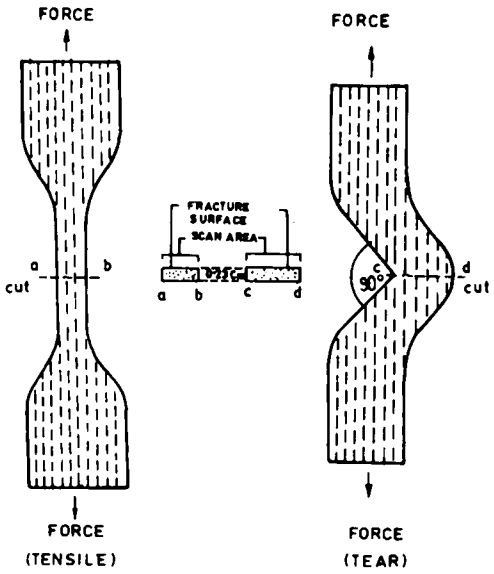

Fig. 4. Fracture surfaces and scan areas.

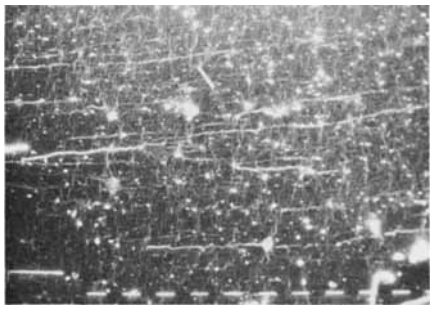

Fig. 5. Photomicrograph of tensile fracture surface of mix S, tear lines (50×).

where the matrix strength is already poor, further weakening of the rubber matrix does not occur with the addition of short fibers. In the case of carbon-black-loaded SBR composites, the matrix strength is high and the weakening of matrix due to addition of short fibers occurs. This is true for jute fiber–carbon black–SBR compositions.

The values of tensile strength of glass fiber–carbon black–SBR composites decrease with the increase in fiber loading. This may be due to the continuous decrease in fiber length with the increase in fiber loading, which reduces the load transfer area between the rubber matrix and the fiber. Anisotropy in tensile strength is observed at higher loadings for both jute and glass fibers. Modulus at 100% elongation increases steadily with the fiber loading and also the anisotropy becomes more evident. It was reported earlier with other fibers that anisotropy was prominent at lower strains.[16]

As expected, tear strength increases, hardness increases, and resilience decreases with the increase in fiber loading. These observations are similar to our earlier observations.[7,11] This has been explained later with the help of SEM studies.

Heat buildup values increase with the increase in fiber loading. It may be because of the increased stiffness associated with increase in fiber loading. It is known that in the case of short fiber-rubber composites the fiber ends are the stress raisers and act as the points of heat generation. With the increase in fiber loading the number of fiber ends per unit volume increases, and hence there is high heat generation. Similar results were obtained earlier.[7,11]

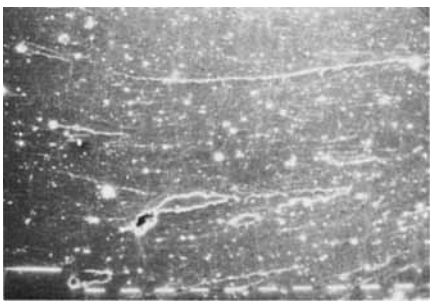

Fig. 6. Photomicrograph of tensile fracture surface of mix T, tear lines (50×).

Fig. 7. Photomicrograph of tensile fracture surface of mix U, cracks (50 ×).

The change in the compression set values are marginal. In general, glass fiber–SBR composites exhibit lower resistance to compression set.

Flex cracking resistance of the composites decreases with the increase in fiber loading. Addition of carbon black causes further deterioration. Since both fibers and carbon black make the composites stiffer, it is expected that flex cracking resistance decreases with increase in stiffness. It is for similar reasons that the flex cracking resistance is better for the composites with fibers aligned transversely.

Abrasion resistance decreases with the increase in fiber loading and addition of carbon black improves the property. The low abrasion resistance of fiber-filled rubber composites is mainly due to loss of fibers.[12]

Volume fraction of rubber in swollen vulcanizates, a measure of reinforcing ability, increases with the increase in fiber loading. Similar results were reported earlier.[20] Comparison of the values for both jute fiber– and glass fiber–SBR composites shows that jute fiber offers better resistance to swelling, indicating higher reinforcing ability of the jute fiber.

Aging retention properties are always better for fiber-reinforced composites as the fibers do not deteriorate on aging. The results are in agreement with our earlier observations.[7,8,11]

Scanning Electron Microscopy Studies. SEM studies are designed in such a way that they could explain the effect of bonding agents, carbon black, jute fiber, and glass fiber on the fracture mode of the vulcanizates. Table V gives the formulations of the mixes used for SEM studies. The fracture surfaces and scan areas are given in Figure 4. Figure 5 shows the photomicrograph of tensile

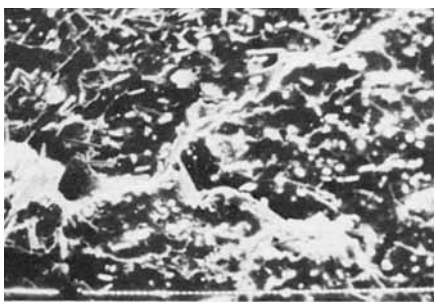

Fig. 8. Photomicrograph of tensile fracture surface of mix V (100 ×).

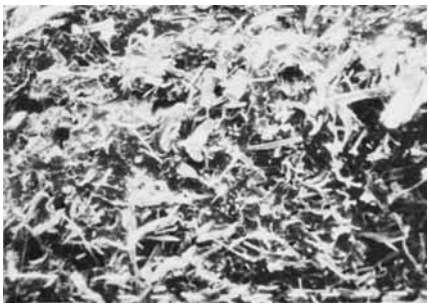

Fig. 9. Photomicrograph of tensile fracture surface of mix W (50 ×).

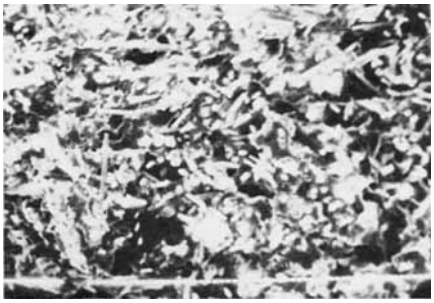

Fig. 10. Photomicrograph of tensile fracture surface of mix X (100 ×).

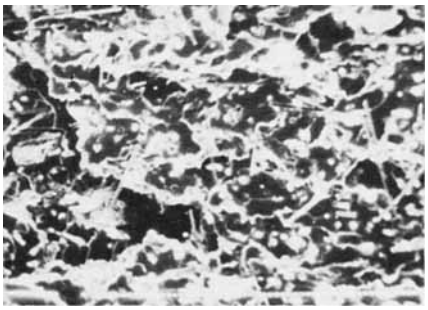

Fig. 11. Photomicrograph of tensile fracture surface of mix Y (100 ×).

fracture of mix S. The surface is smooth and contains short tear lines and ripplings. Addition of carbon black (mix T) increases the roughness of the surface (Fig. 6) and increases the strength of the vulcanizate. The presence of resin (resorcinol and hexa, but no fiber) as in mix U leads to the fracture by the formation of cracks (Fig. 7). Figure 8 gives the tensile fracture surface of glass fiber–SBR composites (mix V). It is clear from the photomicrograph that glass fibers do not cause any obstruction to the fracture propagation, and, consequently, the improvement in strength is not prominent. Similar observations can be obtained from Figure 9, which shows the tensile fracture surface of jute-fiber-reinforced SBR composites (mix W). Since the densities of glass fiber and

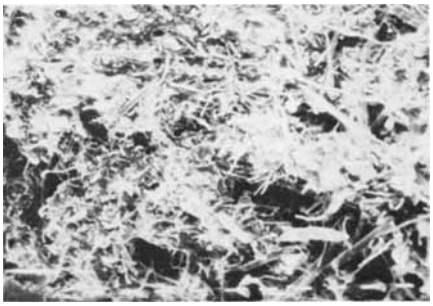

Fig. 12. Photomicrograph of tensile fracture surface of mix Z (100 ×).

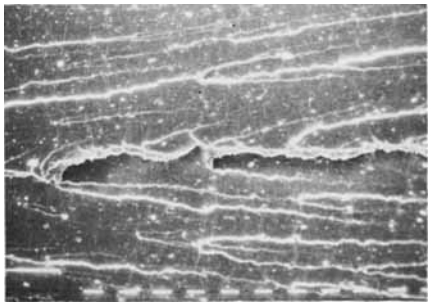

Fig. 13. Photomicrograph of tear fracture surface of mix S (50 ×).

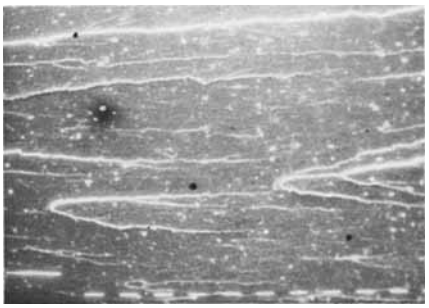

Fig. 14. Photomicrograph of tear fracture surface of mix T (50 ×).

jute fiber are not same, the loading of glass fiber is increased so that mixes W and X contain almost the same volume loading of jute fiber and glass fiber, respectively. As expected, the fracture surface of mix X (Fig. 10) does not differ much from that of mix W (Fig. 9). The matrix is crumpled in the case of mix X because of poor bonding between glass fiber and the rubber matrix. This shows that the nature of fiber does not change the fracture mode. Similar conclusions can be drawn from the photomicrographs of tensile fracture surfaces of mixes Y and Z containing carbon black (Figs. 11 and 12). It is apparent, therefore, that the fracture mode depends much on the adhesion between fiber and matrix rather than on the nature of fiber.

Figures 13, 14, and 15 give the photomicrographs of tear fracture of SBR gum, carbon black filled and resin incorporated mixes (mixes S, T, U), respectively.

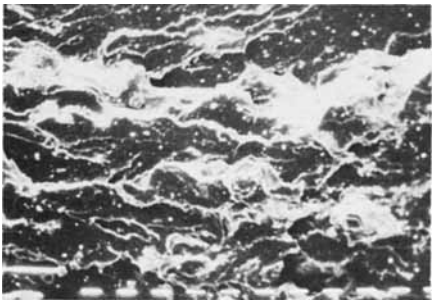

Fig. 15. Photomicrograph of tear fracture surface of mix U (50 ×).

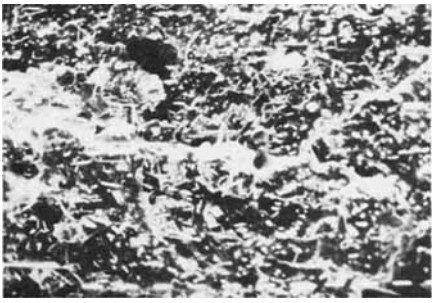

Fig. 16. Photomicrograph of tear fracture surface of mix V (50 ×).

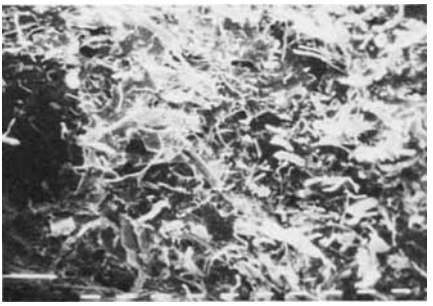

Fig. 17. Photomicrograph of tear fracture surface of mix W (50 ×).

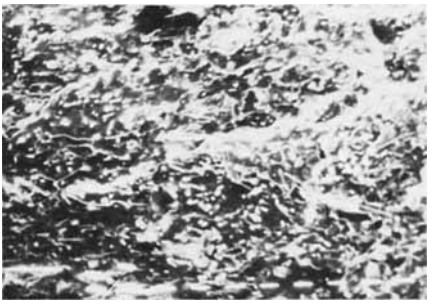

Fig. 18. Photomicrograph of tear fracture surface of mix Y (50 ×).

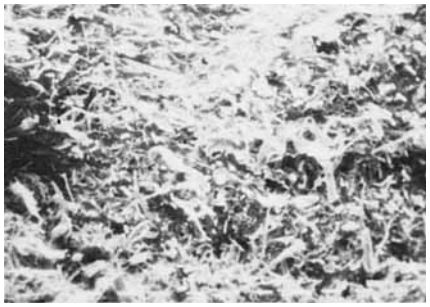

Fig. 19. Photomicrograph of tear fracture surface of mix Z (50 ×).

Mix S fails by the formation of parabolic and long tear lines (Fig. 13). These parabolic tear lines can be considered as produced by the interaction of subsidiary fracture fronts with the main fracture front.[21] Addition of carbon black does not change the fracture mode, but the number of tear lines is less (Fig. 14) and the strength is higher. The tear fracture (Fig. 15) associated with the addition of resin is similar to that of tensile fracture (Fig. 7). From Figures 16 and 17 it can be seen that short fibers obstruct the tear propagation. In the case of jute fiber–SBR composites no tear path can be seen (Fig. 17). Addition of carbon black enhances tear strength and acts similar to the fiber in obstructing tear propagation (Figs. 18 and 19). When the propagating tear comes in contact with the fibers, it may be arrested there or may branch there and proceed. Either of the processes increase the tear strength.

References

1. P. M. Goodloe, T. L. Reiling, and D. H. McMutic, *Rubber Age*, **61**, 697 (1947).
2. J. M. Campbell, *Prog. Rubber Technol.*, **41**, 43 (1978).
3. U. S. Pat. 3,746,669 (1972) (To Monsanto Co.).
4. K. Boustany and R. L. Arnold, *J. Elastoplast.*, **8**, 160 (1976).
5. A. Y. Coran, P. Hamed, and L. A. Goettler, *Rubber Chem. Technol.*, **49**, 1167 (1976).
6. J. E. O'Connor, *Rubber Chem. Technol.*, **50**, 945 (1977).
7. V. M. Murty and S. K. De, *Rubber Chem. Technol.*, **55**, 287 (1982).
8. V. M. Murty and S. K. De, *J. Appl. Polym. Sci.*, **27**, 4611 (1982).
9. S. K. Chakraborty, D. K. Setua, and S. K. De, *Rubber Chem. Technol.*, **55**, 1286 (1982).
10. D. K. Setua and S. K. De, *Rubber Chem. Technol.* **56**, 808 (1983).
11. V. M. Murty, *Int. J. Polym. Mater.* **10**, 145 (1983).
12. V. M. Murty, A. K. Bhowmick, and S. K. De, *J. Mater. Sci.*, **17**, 709 (1982).
13. A. P. Foldi, *Rubber Chem. Technol.*, **49**, 379 (1976).
14. R. Mukhopadhyay, S. K. De, and S. N. Chakraborty, *Polymer*, **18**, 1243 (1978).
15. L. Czarnecki and J. L. White, *J. Appl. Polym. Sci.*, **25**, 1127 (1980).
16. A. Y. Coran, K. Boustany and P. Hamed, *J. Appl. Polym. Sci.*, **15**, 2471 (1971).
17. P. C. Li, L. A. Goettler, and P. Hamed, paper presented at ACS meeting, Chicago, 1977.
18. L. J. Broutman and R. H. Krock, *Modern Composite Materials*, L. J. Broutman and R. H. Krock, Eds., Addison-Wesley, London, 1967, Chap. 1.
19. E. A. Dzyuza, *Int. J. Polym. Mater.*, **8**, 165 (1980).
20. B. Das, *J. Appl. Polym. Sci.*, **17**, 1019 (1973).
21. A. Kadir and A. G. Thomas, *Rubber Chem. Technol.*, **54**, 15 (1981).

Received May 16, 1983
Accepted September 28, 1983